

## ON THE ROLE OF COMPRESSION OVERLOADS IN INFLUENCING CRACK CLOSURE AND THE THRESHOLD CONDITION FOR FATIGUE CRACK GROWTH IN 7150 ALUMINUM ALLOY

E. ZAIKEN† and R. O. RITCHIE

Department of Materials Science and Mineral Engineering, University of California,  
Berkeley, CA 94720, U.S.A.

**Abstract**—A study has been made of the effect of single compression cycles on near-threshold fatigue crack propagation in an *I/M* 7150 aluminum alloy. Based on experiments at a load ratio of  $R = 0.10$  on cracks arrested at the fatigue threshold ( $\Delta K_{TH}$ ) in under-, peak and overaged microstructures, large compression overload cycles, of magnitude five times the peak tensile load, were found to cause immediate reinitiation of crack growth, even though the applied stress intensity range did not exceed  $\Delta K_{TH}$ . Following an initial acceleration, subsequent crack advance was observed to take place at progressively decreasing growth rates until rearrest occurred. Such behavior is attributed to measured changes in crack closure which vary the effective near-tip driving force for crack extension ( $\Delta K_{eff}$ ). Specifically, roughness-induced closure primarily is reduced by the application of compressive cycles via a mechanism involving crack surface abrasion which causes flattening and cracking of fracture surface asperities. Closure, however, is regenerated on subsequent propagation resulting in the rearrest. Such observations provide further confirmation that the existence of a fatigue threshold is controlled principally by the development of crack closure and are discussed in terms of the mechanisms of closure in precipitation hardened alloys.

### INTRODUCTION

THE GENERATION of fatigue crack closure, either from the presence of cyclic plasticity or through microstructural or environmental mechanisms, is now recognized as a major factor contributing to the development of a fatigue threshold, representing the stress intensity range  $\Delta K_{TH}$  below which long cracks appear dormant (see, for example, Refs. [1-11]). Such closure, which results from interference between mating fracture surfaces, serves to reduce the near-tip driving force for crack advance from nominal levels, based on global measurements of applied loads and crack size, e.g.  $\Delta K = K_{max} - K_{min}$ , to some effective level actually experienced at the crack tip, e.g.  $\Delta K_{eff} = K_{max} - K_{cl}$ , where  $K_{cl}$  is the stress intensity on first contact of the crack surfaces during unloading [12]. Moreover, because of the nature of such contact which must occur in the wake of the crack tip, closure forces are limited at high load ratios ( $R = K_{min}/K_{max}$ ) and at high stress intensity ranges due to the larger crack tip opening displacements, and at very small crack sizes due to the restricted wake [11]. The latter aspect appears to be one basis of the "anomalous" behavior of short cracks, which are small compared to the extent of local plasticity or microstructural size-scales or are simply physically small (i.e.  $\approx 1$  mm), as such cracks can initiate and grow, at progressively decreasing growth rates, *below* the long crack threshold with an associated smaller influence of closure [13, 14].

Recently, verification of this hypothesis, that both the existence of a threshold and the subthreshold propagation of short cracks are primarily related to closure phenomena, has been sought using experiments involving removal of material left in the wake of threshold fatigue cracks [15-18]. Through mechanical or electrodischarge machining of the wake of long cracks to within 0.5 to 1 mm of the tip, threshold cracks arrested at  $\Delta K_{TH}$  in both steels [15] and aluminum alloys [16-18] were found to recommence to propagate at  $\Delta K$  levels *not exceeding*  $\Delta K_{TH}$ , consistent with a measured reduction in closure. Moreover, subsequent propagation rates, simulating the growth of short cracks emanating from a notch, were observed to be progressively decelerated consistent with a measured redevelopment of closure with increasing crack length [17, 18]. The location of the closure was determined by monitoring  $K_{cl}$  values during the micromachining process. Such measurements [16-18] indicated that closure far from

†Present address, Shiley Incorporated, Irvine, CA 92714, U.S.A.

the crack tip was relatively less important and that approximately 50% of the closure was confined to within 500  $\mu\text{m}$  or so from the tip.

In the present work, an alternative procedure is investigated for limiting crack closure in the wake of the crack tip. Specifically, the role of single compression overloads in influencing closure and near-threshold behavior of long cracks arrested at  $\Delta K_{\text{TH}}$  is examined in under-, peak and overaged microstructures in an *I/M* 7150 aluminum alloy. Similar to prior experiments involving wake micromachining [18], compression overloads of sufficient magnitude were found to reduce the closure associated with arrested threshold cracks, resulting in an immediate recommencement of growth at  $\Delta K_{\text{TH}}$ .

## BACKGROUND

Whereas compression cycles are often a common occurrence in service, particularly for aerospace applications, and are known to be of importance in the process of crack initiation in smooth specimens, their effect on the propagation of (long) fatigue cracks, at least at intermediate to high  $\Delta K$  levels, has long been considered to be minimal (e.g. Ref. [19]). This is in keeping with standard fracture mechanics concepts which imply that the crack will be closed during the compressive portion of the cycle, necessitating a stress intensity of zero at the tip, and the fact that tests invariably have been performed on long cracks where the magnitude of both tensile and compressive stresses are small. Although data are limited, several authors have found growth rates to be slightly faster at negative load ratios compared to  $R = 0$  in both steels and aluminum alloys [19–25], although the effect is negligible in certain alloys such as 7075-T6 [19]. Under variable amplitude fatigue loading, however, cyclic compressive stresses immediately following tensile overloads are known to lessen the post overload retardation in growth rates which usually accompanies single tensile overloads [26–28]. Moreover, under certain conditions of cracks initiating from notches, fatigue crack growth has been demonstrated under purely cyclic compressive loading [29–32]. In fact the technique has been used as a reliable means of producing small flaws for short crack experiments [30, 31].

Unlike behavior at higher growth rates where effects are small, recent studies at near-threshold levels have highlighted a significant role of compressive cycling on crack extension behavior [22–25]. Not only are threshold  $\Delta K_{\text{TH}}$  values lower at  $R = -1$  compared to  $R = 0$ , but large periodic compressive cycles (of the order of one half the yield stress) applied during positive  $R$  cycling have been shown to dramatically reduce the threshold and to accelerate crack growth rates in both mild steel [25] and 2024-T3 aluminum [24]. Physical explanations for these effects remain unproven, although several suggestions have been proffered including redistribution of residual stresses *ahead* of the crack tip and reduced closure forces due to a diminished deformation zone left *behind* the crack tip [25]. In addition, periods of compression during the fatigue cycle are likely to result in a flattening of fracture surface asperities and a compacting of corrosion debris on crack faces, both processes leading to a reduction in closure via the roughness-induced [6–8] and oxide-induced [3–5] mechanisms, respectively.

The objectives of the current study were to investigate the role of single compression overload cycles on the propagation behavior of cracks arrested at the threshold, and specifically to monitor the variation in crack closure, both macroscopically in terms of  $K_{\text{cl}}$  measurements and microscopically in terms of changes in fracture surface morphology. A precipitation hardened aluminum alloy, 7150, was chosen for the study because in such systems the operative mechanisms of closure can be readily varied by heat treatment [33].

## EXPERIMENTAL PROCEDURES

### *Material*

Tests were performed on a conventionally-cast *I/M* 7150 aluminum alloy, supplied by ALCOA as 25-mm-thick plate in the solution treated and 2% stretched (*W51*) condition. The alloy, of composition shown in Table 1, is a high purity version of 7050 with lower levels of Si and Fe. Samples were machined from quarter and three-quarter plate thickness locations only and tempered to produce underaged, peak aged (*T6*) and overaged (*T7*) conditions. The specific heat treatments, which were designed to yield under- and overaged microstructures with iden-

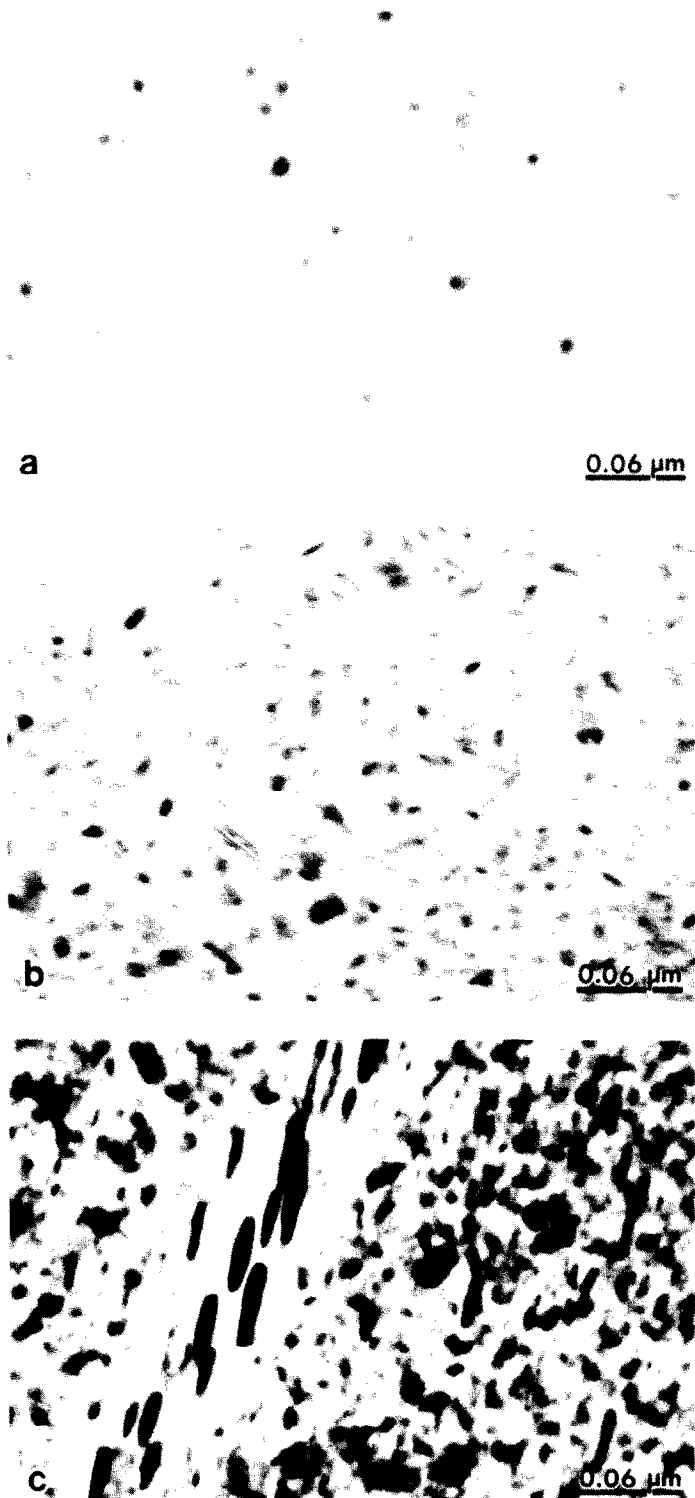


Fig. 1. Transmission electron micrographs of (a) underaged, (b) peak aged (T6) and (c) overaged (T7) *II/M* 7150 aluminum alloy [33].

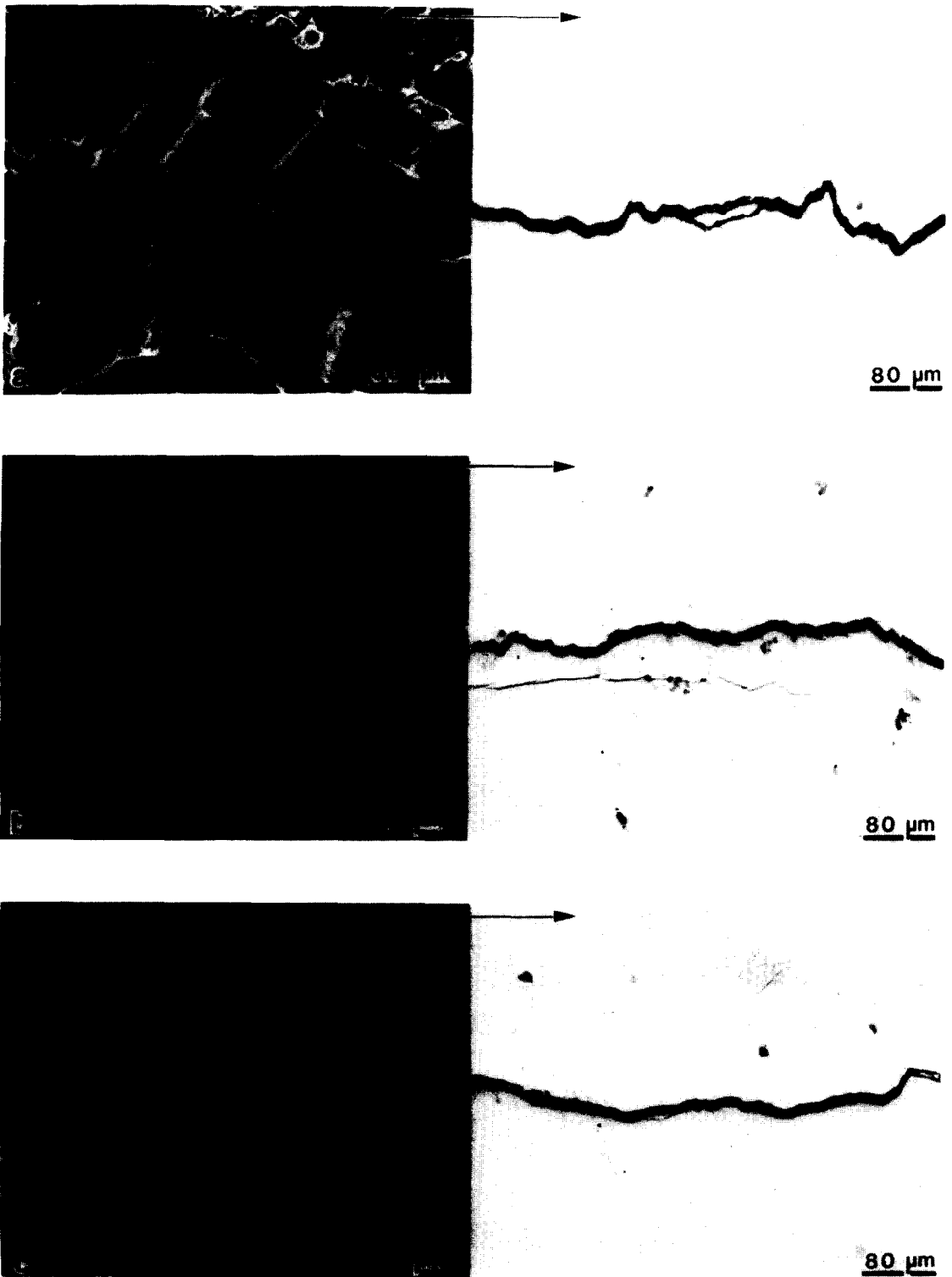


Fig. 6. Fracture surface and crack path morphologies for steady-state fatigue crack growth at near-threshold stress intensities in underaged, peak aged and overaged 7150 aluminum alloy [33]. Arrows indicate general direction of crack growth.

Table 1. Nominal chemical compositions in wt %

	Si	Fe	Cu	Mg	Zn	Ti	Zr	Al
7150	0.07	0.11	2.10	2.16	6.16	0.02	0.13	balance

tical strength levels, are listed in Table 2. Corresponding room temperature mechanical properties are shown in Table 3. Microstructures of the three aging conditions, shown in Fig. 1, have been described elsewhere [33]. Briefly, underaged structures were hardened by small coherent GP zones, roughly 4 to 8 nm in diameter, compared to hardening by semicoherent  $\eta'$  precipitates in peak aged structures. Overaged structures, conversely, showed evidence of coarsened  $\eta'$  precipitates in the matrix and predominately incoherent  $\eta$  precipitates in both matrix and grain boundaries, with small precipitate free zones of roughly 30 nm half-widths. Grains were elongated along the rolling direction with an approximate size of 15 by 5  $\mu\text{m}$ .

### Fatigue testing

Fatigue crack propagation testing was performed in controlled room temperature air (22°C, 45% relative humidity) using 6.4-mm-thick compact  $C(T)$  test pieces machined in the  $T$ - $L$  orientation. Tests were conducted under load control at a frequency of 50 Hz (sine wave) at a load ratio of 0.10. Direct current electrical potential methods were used to continuously monitor crack growth. Corresponding macroscopic crack closure measurements to determine  $K_{cl}$  values were carried out *in situ* using a back-face strain technique employing two strain gauges to record strain both parallel and perpendicular to the loading axis [34]. Mean closure loads were deduced from the point during the unloading cycle when the resulting elastic compliance curves of load versus relative strain first deviated from linearity.

Compression overload experiments were performed by first determining the long crack threshold using manual load shedding cycling, as described elsewhere [35]. In this manner, constant amplitude (steady-state) crack growth data between  $\sim 10^{-6}$  and  $10^{-11}$  m/cycle were obtained under decreasing  $\Delta K$  conditions, with the threshold  $\Delta K_{TH}$  operationally defined as the highest stress intensity range giving growth rates less than  $10^{-11}$  m/cycle. Single (spike) compressive overloads were then applied to cracks arrested at  $\Delta K_{TH}$ . The length of such arrested cracks was of the order 5 to 7 mm beyond the 17.5 mm initial notch in the compact specimen, i.e.  $a \approx 23$  to 25 mm. With the applied loading conditions then maintained at a constant  $\Delta K = \Delta K_{TH}$ , subsequent growth rate and crack closure behavior were monitored closely. The magnitudes of the compression overload cycles were varied between one and five times the maximum tensile load in the fatigue cycle, i.e. up to a maximum compressive load between 1.8 and 2.8 kN corresponding to a fictitious “negative” stress intensity of 12 to 17  $\text{MPa}\sqrt{\text{m}}$ .† The application of the single compression overloads at  $\Delta K = \Delta K_{TH}$  was repeated two or three times on each specimen with at least 200  $\mu\text{m}$  of crack extension between each event.

### Fracture surface analysis

Fatigue fracture surfaces were examined using both optical and scanning electron microscopy. As described elsewhere [33], the degree of fracture surface roughness was assessed from

Table 2. Heat treatments utilized for tests on 7150 alloy

Underaged	ST† + 1½ hr at 121°C
Peak-aged (T6)	ST† + 100 hr at 121°C
Overaged (T7)	ST† + 24 hr at 121°C + 40 hr at 163°C

† ST – solution treated, quenched and stretched 2% (W51 condition)

†As the compact specimen is not ideally suited for the application of compression cycles, such stress intensity values are very approximate and merely give an indication of magnitude of the overloads, i.e.  $\sim 5$  times  $K_{max}$ . Current tests are being performed with center-cracked tension specimens where the magnitude of the compressive stresses and stress intensities are more readily amenable to analysis.

Table 3. Room temperature mechanical properties of 7150 alloy

	Yield strength	U.T.S.	Elong.†	Redn. area	Work hardening exponent
	(MPa)	(MPa)	(%)	(%)	
Underaged	371	485	6.8	12.1	0.055
Peak-aged (T6)	404	480	6.0	10.3	0.046
Overaged (T7)	372	478	7.1	12.5	0.058

† On 32-mm-gauge length.

microstructural sections through crack paths, in terms of the ratio of total length of crack to projected length on the plane of maximum tensile stress. The thickness of crack surface corrosion deposits were measured in the scanning Auger spectroscopy using  $\text{Ar}^+$  sputtering procedures [5, 33].

## RESULTS

### Steady-state fatigue behavior

The variation in fatigue crack propagation rate ( $da/dN$ ) as a function of the nominal stress intensity range ( $\Delta K$ ), at  $R = 0.10$  and  $0.75$ , is shown in Fig. 2 for the under-, peak and overaged microstructures in 7150 alloy under steady-state (nonvariable amplitude) conditions. Data plotted in this figure represent mean values from at least three duplicate tests. Corresponding crack closure data have been presented elsewhere [33] and indicate that the progressively lower threshold values (and higher near-threshold growth rates), which are seen with increased aging, are consistent with less measured closure at  $R = 0.10$ . In all structures,  $K_{cl}/K_{max}$  values increased with decreasing  $\Delta K$ , to approach unity at  $\Delta K_{TH}$ . Relevant threshold data for these microstructures, including the extent of crack surface oxidation and degree of fracture surface roughness, are listed in Table 4 and are described in detail in Ref. [33].

### Compression overload tests

Application of 100 to 300% single (spike) compression overloads (corresponding to one to three times the peak tensile loads) were observed to have no effect on crack closure or crack

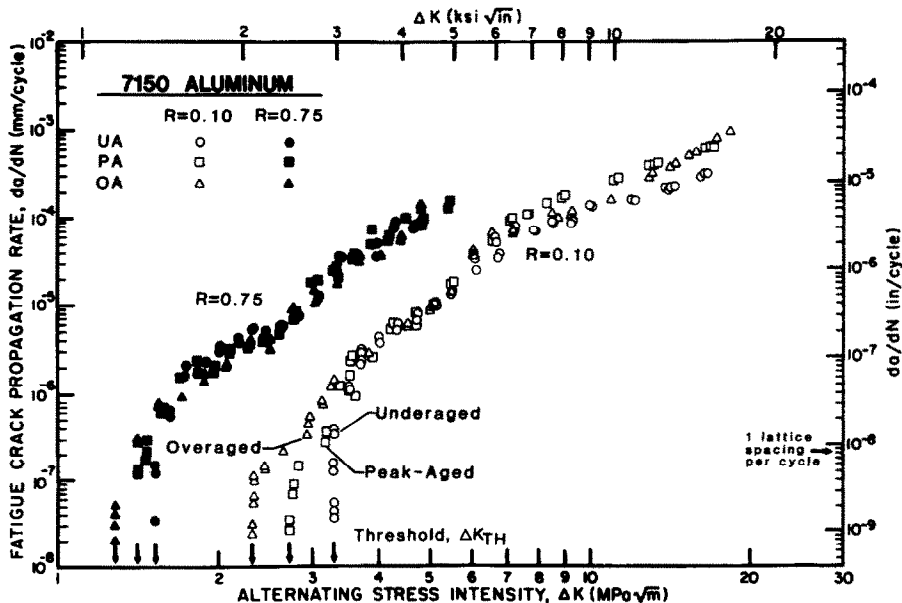


Fig. 2. Variation in steady-state fatigue crack propagation rates ( $da/dN$ ) with stress intensity range ( $\Delta K$ ) for  $I/M$  7150 aluminum alloy tested in controlled moist air at  $R = 0.10$  and  $0.75$ . Data represent the mean results for duplicate tests on long cracks ( $a \approx 25$  mm) in underaged (UA), peak aged (PA) and overaged (OA) structures [33].

Table 4. Threshold data for 7150 alloy at R = 0.10

	Code	$\Delta K_{TH}$ (MPa $\sqrt{m}$ )	Plastic zone size <sup>†,‡</sup>		Excess oxide thickness <sup>†</sup> (nm)	Degree of roughness <sup>§</sup>
			Cyclic ( $\mu m$ )	Maximum ( $\mu m$ )		
Underaged	UA	3.05-3.31	2.9	14.5	~3	1.26
Peak-aged (T6)	PA	2.44-2.94	1.8	8.8	~3	1.21
Overaged (T7)	OA	2.17-2.33	1.5	7.4	~3	1.06

<sup>†</sup> At the threshold,  $\Delta K_{TH}$ .

<sup>‡</sup> Computed from  $r_{\Delta} = \frac{1}{2}\pi (\Delta K/2\sigma_y)^2$  and  $r_{max} = \frac{1}{2}\pi (K_{max}/\sigma_y)^2$  and  $\Delta CTOD = \frac{1}{2}(\Delta K^2/2\sigma_y E)$ , where  $r_{\Delta}$  and  $r_{max}$  are the cyclic and maximum plastic zone sizes and  $\sigma_y$  the yield strength [36].

<sup>§</sup> Ratio of total crack length to projected length on plane of maximum tensile stress (lineal roughness parameter).

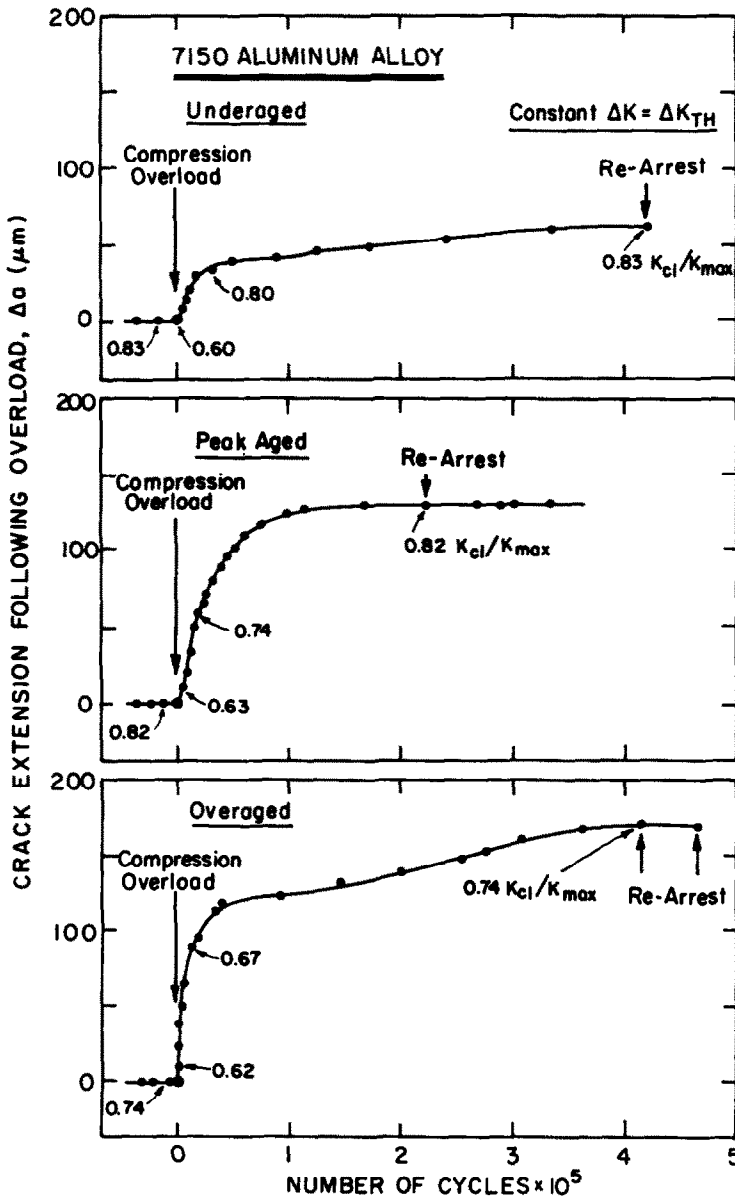


Fig. 3. Fatigue crack extension as a function of the number of cycles following application of 500% compression overloads on arrested threshold cracks in underaged, peak aged and overaged 7150 aluminum alloy. Data obtained under constant  $\Delta K = \Delta K_{TH}$  cycling conditions at R = 0.10.  $K_{cl}/K_{max}$  closure data are listed beneath each curve.

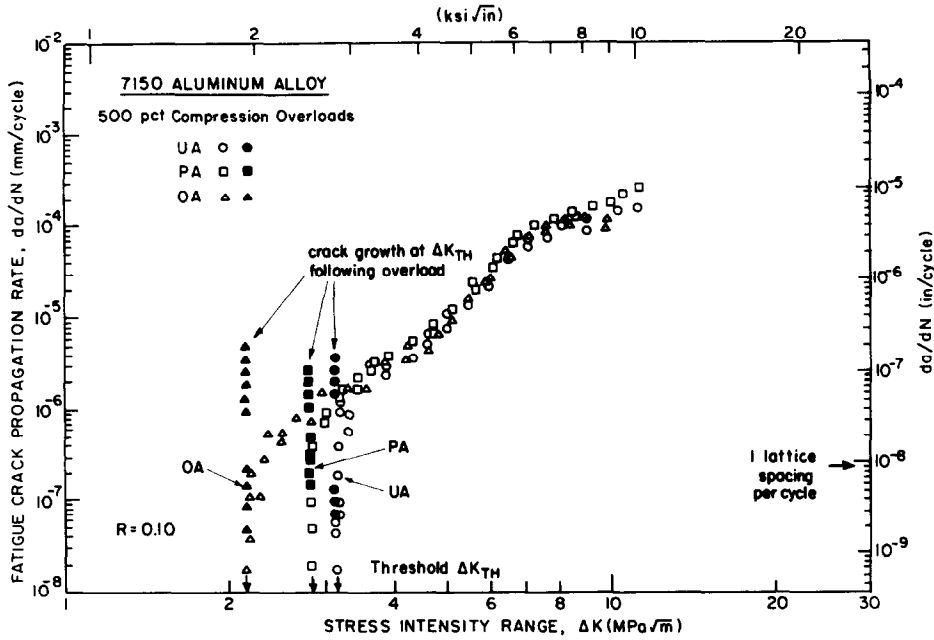


Fig. 4. Fatigue crack growth rate behavior, as a function of nominal stress intensity range ( $\Delta K$ ), for cracks previously arrested at the threshold ( $\Delta K_{TH}$ ) following the application of single 500% compression overloads (solid symbols). Data for underaged (UA), peak aged (PA) and overaged microstructures (OA) in 7150 aluminum alloy are compared with steady-state results from individual tests at  $R = 0.10$  (open symbols).

growth of arrested cracks at the threshold. Crack growth behavior following the application of 500% compression overloads, however, is shown in Fig. 3 for the three microstructures. Here the compressive cycle has been applied and the subsequent closure and growth rates monitored under constant  $\Delta K = \Delta K_{TH}$  cycling conditions. It is clearly apparent that the application of

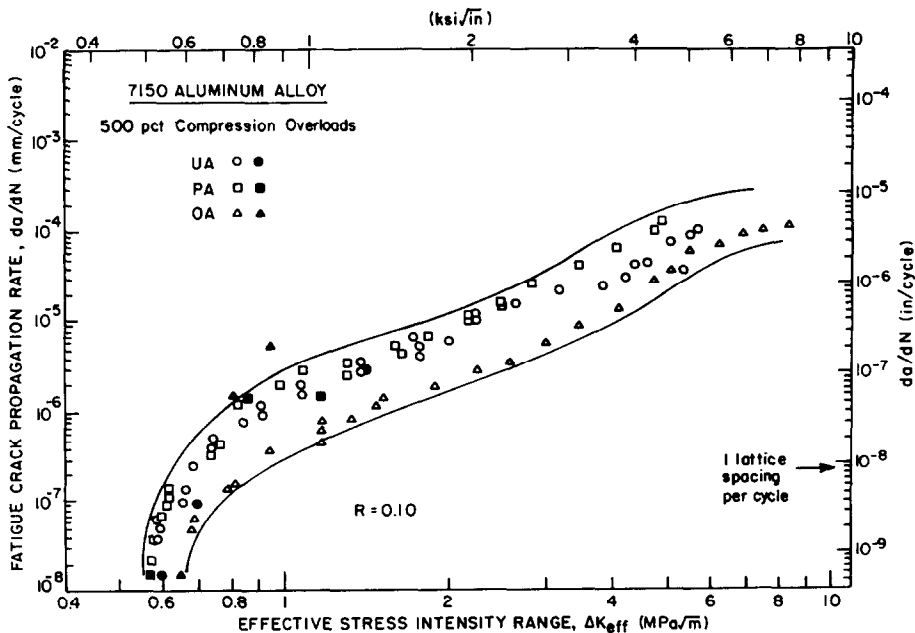


Fig. 5. Fatigue crack growth rates, as a function of the effective stress intensity range ( $\Delta K_{eff}$ ), for both steady-state behavior (open symbols) and following application of 500% compression overloads (solid symbols). Data from Fig. 3 for underaged (UA), peak aged (PA) and overaged (OA) microstructures in 7150 aluminum alloy.  $\Delta K_{eff}$  calculations based on measured closure stress intensity data.

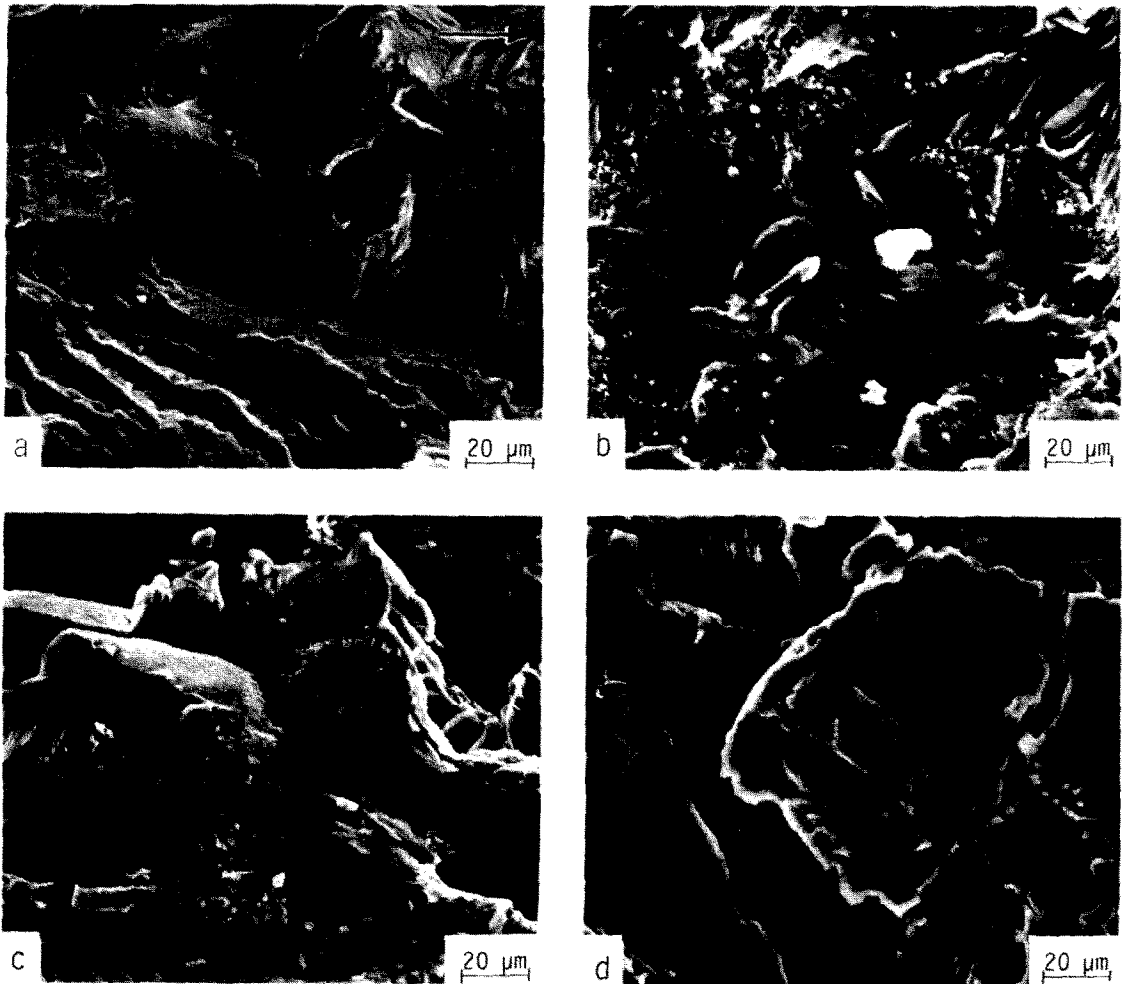


Fig. 7. Scanning electron micrographs of fatigue fracture morphology in underaged 7150 aluminum alloy directly behind the crack tip at the threshold ( $\Delta K \approx 3.2 \text{ MPa}\sqrt{\text{m}}$ ), showing (a) well-defined facets before the application of the compression overload, and (b) fretting oxide debris, (c) asperity flattening and (d) asperity cracking after the application of the overload. Arrow indicates general direction of crack growth.

Table 5. Closure,  $\Delta K_{\text{eff}}$  and crack extension data at  $\Delta K = \Delta K_{\text{TH}}$  before and after compression overloads on arrested cracks

Microstructure	$\Delta K_{\text{TH}}$ (MPa $\sqrt{\text{m}}$ )	At initial arrest		Following overload		At rearrest		Crack ext. to rearrest $\Delta a$ ( $\mu\text{m}$ )
		$K_{\text{cl}}/K_{\text{max}}$	$\Delta K_{\text{eff}}$ (MPa $\sqrt{\text{m}}$ )	$K_{\text{cl}}/K_{\text{max}}$	$\Delta K_{\text{eff}}$ (MPa $\sqrt{\text{m}}$ )	$K_{\text{cl}}/K_{\text{max}}$	$\Delta K_{\text{eff}}$ (MPa $\sqrt{\text{m}}$ )	
Underaged	3.14	0.83	0.59	0.60	1.40	0.83	0.59	60
Peak-aged (T6)	2.81	0.82	0.56	0.63	1.15	0.82	0.56	130
Overaged (T7)	2.17	0.74	0.63	0.62	0.92	0.74	0.63	170

the compressive overload causes immediate propagation of the arrested cracks, even though the stress intensity range does not exceed  $\Delta K_{\text{TH}}$ . Moreover, under such constant  $\Delta K$  conditions, the initial acceleration, to as high as  $\sim 10^{-5}$  mm/cycle, is followed by a progressive deceleration in growth rates until rearrest. The extent of crack growth before rearrest occurs is of the order of 60  $\mu\text{m}$  in the underaged structure, far smaller than in the peak and overaged structures where the crack extends a further 130 and 170  $\mu\text{m}$ , respectively, before arrest. Application of a second single compression overload on the rearrested crack at this stage produced identical results. Such behavior was accompanied by significant changes in the magnitude of the crack closure. The initially high closure values which are associated with the original arrest at the threshold, i.e.  $K_{\text{cl}}/K_{\text{max}}$  values of the order of 0.75–0.85, were reduced

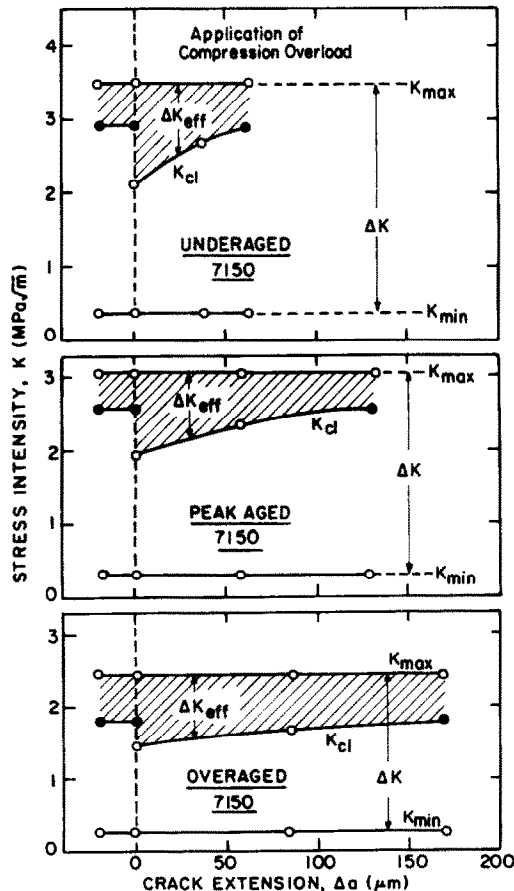


Fig. 8. Variation in  $\Delta K$  and  $\Delta K_{\text{eff}}$  with crack extension, computed from measured  $K_{\text{cl}}$  closure data, for fatigue crack growth behavior in underaged, peak aged and overaged 7150 aluminum alloy following application of single compression overloads on arrested cracks at  $\Delta K = \Delta K_{\text{TH}}$ .

immediately by 16 to 28% to approximately 0.60 by the compressive overload. With further crack extension, however, the closure was regenerated until arrests again occurred at a  $K_{cl}/K_{max}$  level similar to that of the original (pre-overload) threshold. Such closure measurements, together with the corresponding effective stress intensity ranges, i.e.  $\Delta K_{eff}$  values, are listed in Table 5. Plots of the pre- and post-overload growth rates as a function of both nominal and effective stress intensities, computed from these data for individual tests, are shown in Figs. 4 and 5, respectively. It can be seen that the “anomalously” high growth rates at  $\Delta K_{TH}$ , resulting from the application of the compression cycles, fall within the scatterband for steady-state growth rates when characterized in terms of  $\Delta K_{eff}$  rather than  $\Delta K$ . This clearly implies a dominant role of closure.

### Fractography

The fractography of steady-state near-threshold fatigue crack growth in this alloy is summarized in Fig. 6 and has been described in some detail elsewhere [33]. Briefly, at low  $\Delta K$  levels, fracture surfaces show little evidence of corrosion debris and in underaged microstructures tend to be faceted and irregular, compared to the relatively smoother appearance of the peak and overaged structures. In terms of crack path morphology, this can be seen as many instances of crack deflection, in contrast to the more linear profiles in the more heavily aged microstructures. Following compression overload cycles, however, the well-defined features of these fracture surfaces become obscured somewhat. As shown in Fig. 7, there are clear indications of abrasion, compacted fretting oxide debris and the cracking and flattening of fracture surface asperities close behind the crack tip. These features, which always predominated in the immediate vicinity of the crack tip, were profuse in underaged structures where the asperities were most pronounced due to the faceted nature of the crack path.

## DISCUSSION

The present results show a dramatic effect of compression overloads on the propagation behavior of “long” fatigue cracks. The application of a single compression cycle (of magnitude five times the maximum fatigue tensile load corresponding to a nominal bending stress of  $\sim 30\%$  of the yield stress) was seen to result in the “removal” of the fatigue threshold. Moreover, previously arrested cracks at the threshold underwent an instantaneous acceleration in growth rates, to levels approaching  $\sim 10^{-5}$  mm/cycle, even though the applied stress intensity range was maintained constant at  $\Delta K_{TH}$  (Figs. 3 and 4). Such phenomena were accompanied by a measured reduction in crack closure, in the form of decreased  $K_{cl}$  values, and hence can be related to an increase in near-tip crack driving force,  $\Delta K_{eff}$ , following the compression cycle (Table 5).

Mechanistically, the increased local driving force can be attributed to two principal factors. In the present tests, the major effect appears to result from a reduction in roughness-induced closure from a flattening of fracture surface asperities during the compression, as shown in Fig. 7. The associated evidence of compacted fretting corrosion debris and a lack of fine detail on fracture surfaces, which have undergone compression cycles, both indicate marked abrasion between mating crack faces, consistent with such crushing of asperities. A second mechanism involves the residual stress distribution ahead of the crack tip, which must be altered by the large compressive loads. However, this effect of residual stresses *ahead* of the tip, as opposed to the associated closure *behind* the tip, is likely to be far more pronounced when cracks are small and propagating out of a notch (particularly in bend or compact geometries), due the fulcrum loading effect [32] of the notch in compression.

Following the initial post-overload acceleration of the previously arrested cracks at  $\Delta K_{TH}$ , growth rates progressively decelerate until rearrest occurs (Fig. 3). This is accompanied by a measured build up in crack closure with crack extension, approaching pre-overload threshold levels at the rearrest (Table 5). Based on the  $K_{cl}$  measurements, the computed variation in  $\Delta K_{eff}$  with crack extension ( $\Delta a$ ), both prior to and following the overload, is shown in Fig. 8 for the three microstructures examined. Comparison of this figure with the crack length vs number of cycles data in Fig. 3 indicates that the reinitiation and rearrest of the threshold cracks is at least qualitatively consistent with closure-induced changes in the local driving force  $\Delta K_{eff}$ .

Moreover, since the post-overload growth rate data can be brought into close correspondence with the steady-state fatigue data through characterization in terms of  $\Delta K_{\text{eff}}$  instead of  $\Delta K$  (c.f. Fig. 4 and Fig. 5), it would appear that this explanation is quantitatively consistent as well. These calculations imply that the actual threshold for no fatigue crack propagation in under-, peak and overaged 7150 can be defined in terms of a  $\Delta K_{\text{eff}}$  value of approximately  $0.6 \text{ MPa}\sqrt{\text{m}}$  (Table 5).

Comparison of behavior for the three aging treatments in Fig. 3 indicates that the redevelopment of closure with crack extension, following the application of the compression overload, is very dependent upon microstructure. Rearrest, which involves an increase in  $K_{\text{cl}}$  such that  $\Delta K_{\text{eff}}$  is reduced to the threshold value of  $\sim 0.6 \text{ MPa}\sqrt{\text{m}}$ , occurs after crack extensions between 60 and 170  $\mu\text{m}$ , distances that are the order of 5 to 10 grain sizes and are far larger than the size-scales representative of local crack tip plasticity (c.f. maximum and cyclic plastic zone sites in Table 4). Furthermore, it is apparent that significant closure can develop over far smaller amounts of crack extension in the underaged microstructure compared to the more heavily aged conditions. Such results are consistent with the origins of closure in the 7150 alloy [33], which rely at near-threshold levels primarily on microstructural factors rather than on cyclic plasticity or environmental effects. Due to their inhomogeneous mode of deformation (i.e. coarse planar slip) resulting from hardening by coherent (shearable) particles, underaged structures tend to show crack paths which are more crystallographic in nature than in peak and overaged structures [33, 37–41]. This produces rough, faceted fracture surfaces (Fig. 6) which strongly promote roughness-induced closure in these microstructures [33, 37–39]. In contrast, the development of closure with crack extension in peak and overaged structures is far less efficient [18]. Since the roughness-induced mechanism is the principal source of closure in this alloy, the comparatively smoother crack paths, which result from the more homogeneous deformation mode (i.e. wavy slip) arising from incoherent particle hardening, significantly limit the development of closure in the more heavily aged structures [18, 33, 37–39].

The present experiments, on the role of compression overloads in the propagation and subsequent arrest of threshold fatigue cracks, are analogous to prior studies [17, 18] in 7150 on the effect of the mechanical removal of material left in the wake of threshold cracks. Here, the micro-machining away of wake material causes a similar reduction in closure, leading to a recommencement of growth of previously arrested cracks. Subsequent crack extension again is associated with progressively decreasing growth rates (but not in this case complete arrest) as closure is redeveloped over roughly 2 to 10 grain sizes. The difference in the two types of experiment appears to be in the location of the closure which is removed. Whereas micro-machining can only remove closure away from the crack tip vicinity (i.e. reliably no closer than 500  $\mu\text{m}$ ) [18], the nature of the fracture surface damage in Fig. 7 suggests that compression overloads may primarily limit the more important near-tip closure.

This study, as with prior studies [15–18] on the role of wake removal, clearly identifies the existence of a fatigue threshold with the phenomenon of crack closure. Furthermore, the results show that wherever closure is restricted, such as in the present case with the application of large compression cycles, steady-state propagation rate data characterized in terms of  $\Delta K$  can no longer be relied upon to predict crack growth behavior in a given material.

### CONCLUDING REMARKS

Despite early claims to the contrary [19, 27], compressive loading in the form of single (spike) overloads clearly can lead to dramatic increases in fatigue crack growth rates at low stress intensity ranges and most notably *to crack propagation at the threshold*. These results are consistent with the recent work of Topper and his co-workers [24, 25], who found a linear decrease in threshold values with increasing compressive peak stress, and an accentuation of the effect when the compressive overloads were applied more frequently. Such observations serve to highlight the inherent danger of utilizing low load ratio threshold  $\Delta K_{\text{TH}}$  values in engineering design to predict the absence of fatigue cracking. The existence of the threshold is linked intimately to the degree of closure which controls the effective near-tip driving force, yet such considerations are not incorporated into nominal stress intensity calculations used in defect-tolerant life prediction analyses. Thus, wherever the extent of crack closure is restricted,

such as at high load ratios [2–5], with small flaws or cracks at notches [13–15], or in the presence of large compressive stresses, the consequent increase in near-tip crack driving force can lead to accelerated and nonunique [42] growth rate behavior and, more importantly, to *crack extension at  $\Delta K$  levels at or below the  $\Delta K_{TH}$  threshold.*

## CONCLUSIONS

Based on a study on the effect on single (spike) compression overloads on near-threshold fatigue crack propagation at  $R = 0.10$  in underaged, peak aged and overaged *I/M* 7150 aluminum alloy, the following conclusions can be made:

1. A single compression overload, of magnitude five times the tensile peak load, resulted in immediate reinitiation of growth of cracks arrested at the fatigue threshold even though the applied  $\Delta K$  was maintained constant at  $\Delta K_{TH}$ , consistent with a measured 16 to 28% reduction in crack closure.

2. The reduction in closure stress intensity ( $K_{cl}$ ) following the compressive cycle was related primarily to a reduced contribution from roughness-induced crack closure arising from abrasion between mating crack surfaces, i.e. fractographically to the flattening and cracking of fracture surface asperities in the vicinity of the crack tip.

3. Crack growth at  $\Delta K = \Delta K_{TH}$  following the application of the overload was characterized by a progressive deceleration until rearrest occurred within 60 to 170  $\mu\text{m}$ . Such behavior was accompanied by a measured increase in crack closure back to original pre-overload threshold levels.

4. Compared to the more heavily aged structures, deceleration and rearrest occurred after far less crack extension in underaged microstructures, consistent with a larger magnitude, and more efficient redevelopment, of roughness-induced crack closure. This arises from the coherent particle hardening mechanism in this microstructure which induces a planar slip mode of deformation, thereby promoting rougher, more faceted crack path morphologies and the consequent generation of more pronounced fracture surface asperities.

*Acknowledgements*—This work was funded under Grant AFOSR 82-0181 from the U.S. Air Force Office of Scientific Research with Dr A. H. Rosenstein as Contract Monitor. The authors wish to thank Dr Weikang Yu, Patsy Doneho and Don Krieger for their experimental assistance, the Aluminum Company of America for provision of material and the ALCOA Foundation for additional support.

## REFERENCES

- [1] P. C. Paris, R. J. Bucci, E. T. Wessel, W. G. Clark and T. R. Mager, Extensive study of low fatigue crack growth rates in A533B and A508 steels. *Stress Analysis and Growth of Cracks*, *ASTM STP* **513**, 141–176 (1972).
- [2] R. A. Schmidt and P. C. Paris, Threshold for fatigue crack propagation and effects of load ratio and frequency. *Progress in Flaw Growth and Fracture Toughness Testing*, *ASTM STP* **536**, 79–93 (1973).
- [3] R. O. Ritchie, S. Suresh and C. M. Moss, Near-threshold fatigue crack growth in 2½Cr-1Mo pressure vessel steel in air and hydrogen. *J. Engng Mater. Technol. Ser. H* **102**, 293–299 (1980).
- [4] A. T. Stewart, The influence of environment and stress ratio on fatigue crack growth at near-threshold stress intensities in low-alloy steels. *Engng Fracture Mech.* **13**, 463–478 (1980).
- [5] S. Suresh, G. F. Zamiski and R. O. Ritchie, Oxide-induced crack closure: An explanation for near-threshold corrosion fatigue crack growth behavior. *Metall. Trans. A* **12A**, 1435–1443 (1981).
- [6] N. Walker and C. J. Beevers, A fatigue crack closure mechanism in titanium. *Fatigue Engng Mater. Struct.* **1**, 135–148 (1979).
- [7] K. Minakawa and A. J. McEvily, On crack closure in the near-threshold region. *Scripta Met.* **15**, 633–636 (1981).
- [8] S. Suresh and R. O. Ritchie, A geometric model for fatigue crack closure induced by fracture surface roughness. *Metall. Trans. A* **13A**, 1627–1631 (1982).
- [9] P. K. Liaw, T. R. Leax, R. S. Williams and M. G. Peck, Near-threshold fatigue crack growth behavior in copper. *Metall. Trans. A* **13A**, 1607–1618 (1982).
- [10] W. W. Gerberich, W. Yu and K. Esaklul, Fatigue threshold studies in Fe, Fe-Si and HSLA steel. I. Effect of strength and surface asperities on closure. *Metall. Trans. A* **15A**, 875–888 (1984).
- [11] S. Suresh and R. O. Ritchie, Near-threshold fatigue crack propagation: A perspective on the role of crack closure, in *Fatigue Crack Growth Threshold Concepts* (Edited by D. L. Davidson and S. Suresh), pp. 227–261. TMS-AIME, Warrendale, PA (1984).
- [12] W. Elber, The significance of fatigue crack closure. *Damage Tolerance in Aircraft Structures*, *ASTM STP* **486**, 230–242 (1971).
- [13] J. Schijve, Differences between the growth of small and large fatigue cracks in relation to threshold  $K$  values, in *Fatigue Thresholds* (Edited by J. Bäcklund, A. Blom and C. J. Beevers), Vol. 2, pp. 391–408. EMAS Ltd., Warley, England (1982).

- [14] S. Suresh and R. O. Ritchie, The propagation of short fatigue cracks. *Int. Met. Rev.* **25**, 445–476 (1984).
- [15] J. L. Breat, F. Mudry and A. Pineau, Short crack propagation and closure effects in A508 steel. *Fatigue Engng Mater. Struct.* **6**, 349–358 (1982).
- [16] K. Minakawa, J. C. Newman, Jr. and A. J. McEvily, A critical study of the crack closure effect on near-threshold fatigue crack growth. *Fatigue Engng Mater. Struct.* **6**, 359–365 (1983).
- [17] E. Zaiken and R. O. Ritchie, On the location of crack closure and the threshold for fatigue crack growth. *Scripta Met.* **18**, 847–850 (1984).
- [18] E. Zaiken and R. O. Ritchie, On the development of crack closure and the threshold condition for short and long fatigue cracks in 7150 aluminum alloy. *Metall. Trans. A* **16A**, in review.
- [19] C. M. Hudson and J. T. Scardina, Effect of stress ratio on fatigue crack growth in 7075-T6 aluminum alloy sheet. *Engng Fracture Mech.* **1**, 429–446 (1969).
- [20] T. R. Gurney, The effect of mean stress and material yield stress on fatigue crack propagation in steels. *Metal Constr.* **1**, 91–96 (1969).
- [21] R. P. Skelton and J. R. Haigh, Fatigue crack growth rates and thresholds in steels under oxidizing conditions. *Mater. Sci. Engng* **36**, 17–25 (1978).
- [22] S. Usami, Applications of threshold cyclic-plastic-zone-size criterion to some fatigue limit problems, in *Fatigue Thresholds* (Edited by J. Bäcklund, A. Blom and C. J. Beevers), Vol. 1, pp. 205–238. EMAS Ltd., Warley, England (1982).
- [23] A. F. Blom, A. Hadrboletz and B. Weiss, Effect of crack closure on near-threshold crack growth behaviour in a high strength Al-alloy up to ultrasonic frequencies, in *Mechanical Behavior of Materials IV*, Proc. 4th Intl. Conf. (Edited by J. Carlsson and N. G. Olhsen), Vol. 2, pp. 755–763. Pergamon Press, Oxford (1984).
- [24] P. Au, T. H. Topper and M. L. El Haddad, The effects of compressive overloads on the threshold stress intensity for short cracks, in *Behavior of Short Cracks in Airframe Components*, AGARD Conf. Proc. No. 328, pp. 11.1–11.17. AGARD, France (1983).
- [25] T. H. Topper, M. T. Yu and P. Au, The effects of stress cycle on the threshold of a low carbon steel, in *Proc. VIII Inter-American Conf. on Materials Technology*, San Juan, Puerto Rico, pp. 26.15–26.22 (1984).
- [26] J. Schijve and D. Broek, Crack-propagation tests based on a gust spectrum with variable amplitude loading. *Aircraft Engng* **34**, 314–316 (1962).
- [27] T. M. Hsu and W. M. McGee, Effects of compressive loads on spectrum fatigue crack growth rate. *Effect of Load Spectrum Variables in Fatigue Crack Initiation and Propagation*, ASTM STP **714**, 79–90 (1980).
- [28] D. Gan and J. Weertman, Crack closure and crack propagation rates in 7050 aluminum. *Engng Fracture Mech.* **15**, 87–106 (1981).
- [29] C. N. Reid, K. Williams and R. Hermann, Fatigue in compression. *Fatigue Engng Mater. Struct.* **1**, 267–270 (1979).
- [30] S. Usami and S. Shida, Elastic-plastic analysis of the fatigue limit for a material with small flaws. *Fatigue Engng Mater. Struct.* **1**, 471–481 (1979).
- [31] J. F. McCarver and R. O. Ritchie, Fatigue crack propagation thresholds for long and short cracks in René 95 nickel-base superalloy. *Mater. Sci. Engng* **55**, 63–67 (1982).
- [32] S. Suresh, unpublished research, University of California, Berkeley (1983).
- [33] E. Zaiken and R. O. Ritchie, Effects of microstructure on fatigue crack propagation and crack closure behavior in aluminum alloy 7150. *Mater. Sci. Engng*, **68**, (1985).
- [34] V. B. Dutta, S. Suresh and R. O. Ritchie, Fatigue crack propagation in dual-phase steels: Effects of ferritic-martensitic microstructures on crack path morphology. *Metall. Trans. A* **15A**, 1193–1207 (1984).
- [35] R. O. Ritchie, Near-threshold fatigue crack propagation in steels. *Int. Met. Rev.* **20**, 205–230 (1979).
- [36] C. F. Shih, Relationships between the  $J$ -integral and the crack opening displacement for stationary and extending cracks. *J. Mech. Phys. Solids* **29**, 305–330 (1981).
- [37] M. C. Lafarie-Frenot and C. Gasc, The influence of age-hardening on fatigue crack propagation behaviour in 7075 aluminum alloy in vacuum. *Fatigue Engng Mater. Struct.* **6**, 329–344 (1983).
- [38] S. Suresh, A. K. Vasudévan and P. E. Bretz, Mechanisms of slow fatigue crack growth in high strength aluminum alloys: Role of microstructure and environment. *Metall. Trans. A* **15A**, 369–379 (1984).
- [39] R. D. Carter, E. W. Lee, E. A. Starke and C. J. Beevers, The effect of microstructure and environment on fatigue crack closure of 7475 aluminum alloy. *Metall. Trans. A* **15A**, 555–563 (1984).
- [40] E. Hornbogen and K.-H. Zum Gahr, Microstructure and fatigue crack growth in a  $\gamma$ -Fe-Ni-Al alloy. *Acta Metall.* **24**, 581–592 (1976).
- [41] J. Lindgkeit, A. Gysler and G. Lütjering, The effect of microstructure on the fatigue crack propagation behavior of an Al-Zn-Mg-Cu alloy. *Metall. Trans. A* **12A**, 1613–1619 (1981).
- [42] R. O. Ritchie and S. Suresh, The fracture mechanics similitude concept: Questions concerning its application to the behavior of short fatigue cracks. *Mater. Sci. Engng* **57**, L27–L30 (1983).